Real-Time Pricing Control on Generation-Side: Optimal Demand-Tracking Model and Information Fusion Estimation Solver

Zhi-Yu Xu, Wei-Sheng Xu, Wei-Hui Shao, and Zheng-Yang Zeng

***Abstract*—This paper develops the information fusion based pricing control (IFPC) scheme for the generation-side in the liberalized wholesale electricity market. The market mechanism is described by a feedback system, in which the independent system operator (ISO) interacts with generation companies (GenCOs) via proposing and responding to real-time nodal prices. The linear constrained quadratic optimal tracking problem is formulated; and the solution (nodal price sequence) is repeatedly computed by fusing the recently available information with backward manner and updated over the receding preview horizon. So that the total supply dynamically tracks the demand, the price is stationarized and each GenCO gains the maximal profit for the given price. Numeric results on a 118-bus network validate IFPC's effectiveness and flexibility on incorporating various line rating constraints as well as wind power fluctuation uncertainties. Comparative study demonstrates that IFPC outperforms the negotiated predictive dispatch but elapsing heavier computations. The irrational behavior analysis verifies the convergence to equilibrium; and speculation behavior of GenCOs in the real market is also discussed. Along with the rapid development of smart grid, IFPC is practically enabled by the information and communication technology (ICT); its significance and potentials for renewable energy sources (RES) integration would be realized and exploited.**

***Index Terms*—Information fusion, liberalized electricity market, pricing control, profit maximization, quadratic optimal tracking problem, receding preview horizon.**

NOMENCLATURE

ISO	Independent system operator.
GenCO	Thermal-power generation company.
W-GenCO	Wind-power generation company.
DisCO	Distribution company.
PTU	Preview time unit.

Manuscript received November 21, 2012; revised February 19, 2013, May 15, 2013, August 05, 2013, and November 06, 2013; accepted December 20, 2013. Date of publication January 13, 2014; date of current version June 16, 2014. This work was supported by the National Natural Science Foundation of China under Grant No. 71090404, 91024023 and the Doctoral Program Foundation of Higher Education of China under Grant no. 20130072110045. Paper no. TPWRS-01203-2012.

The authors are with the School of Electronics and Information Engineering, Tongji University, Shanghai 201804, China. (e-mail: xuzhiyu@tongji.edu.cn; icslab2@tongji.edu.cn; shaoweihui@126.com; zengzhengyang@yahoo.com).

Color versions of one or more of the figures in this paper are available online at http://ieeexplore.ieee.org.

Digital Object Identifier 10.1109/TPWRS.2013.2296809

$\mathcal{B}, \mathcal{L}, \mathcal{D}, \mathcal{G}, \mathcal{W}$	Set of bus, line, demand, GenCO, and W-GenCO, respectively.
i	As subscript, index of bus, line, GenCO, W-GenCO, etc.
k	As superscript in bracket, index of PTU.
k_{f}	Preview time horizon in PTUs.
n, n_{L}	Number of bus, line in the network.
T	PTU time.
$\boldsymbol{u}, \boldsymbol{x}, \boldsymbol{x}_{\mathrm{W}}, \boldsymbol{x}_{\mathrm{D}}, \boldsymbol{x}_* \in \mathbb{R}^n$	vector of nodal price, GenCO generation, W-GenCO generation, user demand, and net demand, respectively $(\boldsymbol{x}_{\mathrm{D}} - \boldsymbol{x}_{\mathrm{W}} = \boldsymbol{x}_*)$.
$\boldsymbol{\psi} \in \mathbb{R}^{n_{\mathrm{L}}}$	Vector of line flow.
$\bar{\psi}_{\mathrm{L}i}$	Flow rating of Line i.
y	Total supply by GenCOs, $y = \sum_{i \in \mathcal{G}} x_i$.
y_*	Net demand for GenCOs, $y_* = \sum_{i \in \mathcal{D}} x_{*i} - \sum_{i \in \mathcal{W}} x_{*i}$.
$Q, \boldsymbol{R}, \boldsymbol{S}$	Weight in the objective function and the inverse matrix of corresponding variance in information fusion estimation. Respectively associated to the power imbalance, nodal prices, line flows.
$\boldsymbol{\chi} \in \mathbb{R}^n$	State to be measured and estimated.
$\mathfrak{F}[\hat{\boldsymbol{\chi}}]$	Information of state $\hat{\boldsymbol{\chi}}$.
$\mathfrak{F}[\boldsymbol{\zeta}_i]$	Information of measurement $\boldsymbol{\zeta}_i$.
$\mathfrak{F}[\boldsymbol{\zeta}_i \vert \hat{\boldsymbol{\chi}}]$	Information of state $\hat{\boldsymbol{\chi}}$ from measurement $\boldsymbol{\zeta}_i$.
$q, \boldsymbol{r}, \boldsymbol{s}, \boldsymbol{p}$	White noise sequences with variance $Q^{-1}, \boldsymbol{R}^{-1}, \boldsymbol{S}^{-1}, \boldsymbol{P}^{-1}$, respectively.

I. INTRODUCTION

THE significance of the power system for humanity could never be overstated. But it is nontrivial to operate the power system reliable and efficient [1]. In the context of power industry restructuring, monopolies are replaced by competitive markets, utilities are deregulated to be autonomous generation companies (GenCOs) and distribution companies (DisCOs), respectively, and the dispatch control center is transformed to the market coordinator: independent system operator (ISO) [2]. As illustrated

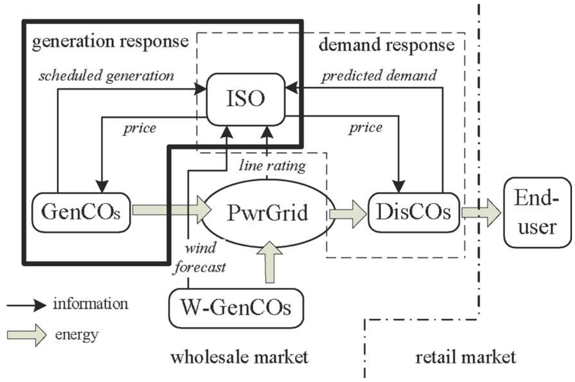

Fig. 1. Structure and interactions of the electricity market.

by Fig. 1, GenCOs produce and sell electricity to DisCOs in the wholesale market. DisCOs buy electricity in the wholesale market, then re-price and sell it to end-users in the retail market. ISO operates the market and maintain the system reliability.

The price plays a crucial role in the electricity market since the "*generation and load profiles are both functions of price offered*" [3], then leads to the idea of pricing control. Through observing the fluctuating price signal [4], [5], GenCOs (generation-side) and DisCOs (demand-side) are respectively willing to modify their energy production and consumption behaviors, so as to maximize the profit of their own.[1] As a sequel, it is possible for the ISO to obtain the required trajectories of generation/demand by applying the proper prices to GenCOs/DisCOs. Thus the technical requirements of the power system and economical optimum of individual could be simultaneously achieved.

The demand-side response (DR), which is shown in the dashed box in Fig. 1, provides benefits to both customers and the system, in the form of electricity bills reduction, congestion relief, capacity requirement mitigation, utilization and reliability improvement, etc. Nevertheless DR still has the inherent weaknesses and limitations [6], [7]. 1) DR's effect is less predictive. Great uncertainties are involved during the load profile aggregation of a *huge number* of *small-capacity* end-users (industrial, commercial, residential, etc.). 2) DR is less capable of addressing the reactive power. Most end-users are owners of various active power appliances; they could change their consumption patterns to balance the active power, but could do little when the reactive power is unbalanced. 3) DR requires initial and running costs on sophisticated infrastructures (smart appliances, metering, communication), the rescheduling of activities, the reduction of comfort, etc. 4) DR faces the regulatory barriers and inappropriate market structures for widely implementation, e.g., the lack of adequate incentives or stable funding mechanism for demand-side resources.

To the contrary, the generation-side response (GR), which is shown in the solid box in Fig. 1, is immune to such problems. 1) GR's effect is more predictive since it is provided by a *small number* of *large-capacity* thermal generators and each generator's output is precisely controllable. 2) GR is capable of tackling not only the active power but also the reactive power, as the synchronous machine could provide both of them. 3) GenCOs could easily afford the investment and running cost associated with GR. 4) The energy market for the generation-side is more developed and relatively mature.

Actually, neither DR nor GR could address all the problems in the future electricity market. It would be more effective to coordinate the DR with GR, and to apply the pricing control on both generation-side and demand-side. However, it is reasonable to separately discuss GR and DR because of the ultra-complexity of the power system. In most articles on DR [8]–[11], only the interactions between the ISO and DisCOs are studied, the scheduled generation is treated as the exogenous input which is unrelated to the electricity price. Adopting the similar methodology, this paper concentrates on the pricing control for generation-side, investigates the dynamics between the ISO and GenCOs, and assumes the predicted demand as the exogenous input which is independent of the prices applied on GenCOs. Notice that such assumption is compatible with cases of DR, because in the viewpoint of GR, the concern is to accurately track the predicted demand, no matter the predicted demand is price-inelastic or has responded to the price. In the following text, unless otherwise noted, we use the term "pricing control" to specify the pricing control on generation-side.

The existing day-ahead market could be viewed as the pricing control based on the hourly market clearing prices (MCPs) which are calculated for each hour of the next operating day [4]. Due to the oligopoly nature of the electricity market, major GenCOs may perform strategic bidding to affect MCP [12]. Considering the inherent feedback dynamics in bidding process, [13] proposes a novel idea which formulates competitive bidding as a feedback system. A PI controller is developed to ensure the power balance in steady state meanwhile each GenCO gains maximal profit. Utilizing as the discrete-time linear model of the bidding process, [14] develops four expectation methods to estimate the rivals' behavior and numerically investigates the output equilibrium and price convergence. Reference [15] examines the controllability and observability of the system. Reference [16] emphasizes the advantage of long term optimization and demonstrates that GenCO could obtain more profit by applying multi-period optimization. To summarize, these works 1) take the viewpoint of GenCO; 2) assume the steady-state power balance; 3) assume the coefficients of demand function are fixed known [13]–[15] or periodically predictable in the hour timescale [16]; and 4) attempt to assist GenCO to bid optimally. In these models, each GenCO is the "controller" which observes the price and makes decision on generation quantity to maximize the profit.

The current trend of the smart grid have stirred research activities from day-ahead MCP to real-time pricing, in which the price dynamically varies to reflect the temporal/spatial value of the electric power in real time [17]. The smart grid has the advantages of strong network structure, flexible power generation, large-scale renewable energy sources (RES) absorption, and intensive real-time interactions through information and communication technology (ICT) [18]. Thus the real-time pricing control is the suitable mechanism for running the electricity market under smart grid.

[1]Although W-GenCOs are also the price responsive market players, they are not taken into account in this paper because the wind power is the clean energy and we attempt to make the maximal use of it. It would be unwise to reduce W-GenCOs' output by applying pricing control on them.

Firstly, the real-time pricing control is effective for mitigating the RES' uncertainties. The RES (wind, solar, biomass, etc.) is intermittent thus less predictable in long term [19]. However in the day-ahead market, both generation profiles and MCP are predetermined by 24 h in advance, thus GenCOs lack enough motivations to frequently modify their settled schedules to cope with the RES fluctuation. If the real-time price is applied, GenCOs would be financially encouraged to respond to the varying price, as well as the fluctuating RES. So that the instantaneous power balance is achieved and quantities of RES are seamlessly integrated into the market.

Secondly, the real-time pricing control is practically enabled by ICT [20]. The ICT allows more connection, automation, and coordination of GenCOs [21]. With the support of the advanced metering infrastructure (AMI), two-way-high-speed communication infrastructure and the decentralized monitoring control programs, the price signals could be broadcast in real-time to GenCOs, and each GenCO could respond to the price in real-time by running the intelligent control software.

Consider the necessity, urgency and feasibility, the real-time pricing control has been recognized as an extremely promising research field. But its exploration still remains a challenging task, mainly due to deriving the "proper" price by comprehensive information incorporation and fusion regarding the behavioral complexity (network topology, generation characteristics, etc.), physical constraints (global power balance, line ratings, etc.) and external uncertainties (demand prediction, wind forecast, etc.). This topic attracts worldwide research interests of renowned institutions, such as MIT [17], [22], ETH [23], [24], TU/e [8], [25], Georgia Tech [26], UC Berkeley [27], etc. Reference [26] designs a spot pricing mechanism for electric utilities to induce SPPFs (small power producing facilities) the desired change of their generation schedules. Reference [28] establishes a decomposition model and separates the spot price for active and reactive power. References [29] and [30] present the real-time nodal price control scheme for power balancing and congestion management, in which the line flow constraints in steady-state and transient are both taken into account. However the nodal demand is assumed fixed or a single step change while the optimization is carried out over a network of several nodes rather than over a time horizon. Thus the solution is multi-node spatial optimum in steady-state instead of multi-period temporal optimum over planning horizon. Reference [23] presents a pricing mechanism respecting wind power integration by applying the receding horizon method of model predictive control (MPC), making more responsive GenCOs to incorporate the real-time variant wind power. Reference [31] further extends MPC to the non-centralized version. The European Union has launched the "E-PRICE" project in 7th Framework Program, aiming to develop novel and feasible pricing control concepts for operating the electricity market powered by smart grid [32].

On the basis of the aforementioned works, we develop the scheme of information fusion based pricing control (IFPC), in which the ISO and GenCOs interact with each other via proposing and reacting on the real-time nodal prices. The main contributions of our work are as follows: 1) The constrained optimal tracking problem is formulated to describe the power network's behavior. The receding preview horizon is applied for price update by incorporating the latest wind forecast. 2) For the first time, the multi-source information fusion approach is introduced to the field of real-time pricing control, so that the overall information is comprehensively integrated. 3) The effectiveness and feasibility of applying IFPC for the real-time computation of price over the large-scale network are verified. The economical benefits of adopting IFPC for the ISO and GenCOs are numerically investigated.

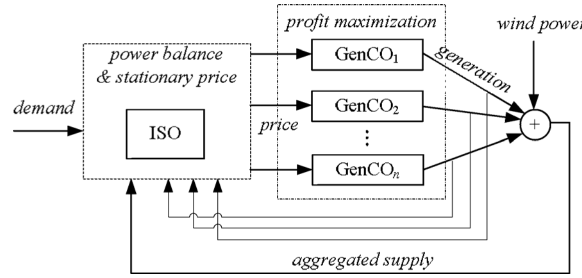

Fig. 2. Block diagram of pricing control for demand tracking.

In the reminder of this paper, Section II formulates the unified scheme of IFPC concerning line ratings and wind power integration. Section III applies the information fusion estimation to derive the optimal pricing law. Sections IV, V and VI present the experimental setup, case study and comparison results, respectively. The irrational and speculative behaviors in the real electricity market are explored in Section VII. Finally Section VIII concludes the paper and proposes perspectives for the future works.

II. Model of Pricing Control

A. ISO-GenCOs Interactive Mechanism

The real-time pricing control of the electricity market is an optimization problem that the global objectives need to be pursued through the actions of individual competing agents; but each agent is interested only in its own profit [33]. The principle of pricing control is depicted by a closed-loop feedback system in Fig. 2. In the system, the ISO is the MIMO (multiple input multiple output) controller which reacts on the market changes and proposes the price to affect GenCOs' behaviors. Its input information includes the predicted user demand, GenCOs' supplies, wind power forecast, etc.; its output signal is the nodal price. All GenCOs constitute the plant. The input is the ISO-offered price and output is the power generation quantity. At each *preview time unit* (PTU), the ISO proposes the proper price sequence over several PTUs in the future (defined as the *preview time horizon*). Considering the ISO-offered price and its own current generation status, each GenCO chooses the proper generation quantity, which could maximize its profit, as the actual output of next PTU. ISO attempts to maintain the supply-demand balance and regulate the electricity price; GenCOs aim to maximize their own profit. Therefore it is necessary to investigate the feasibility of compromising/integrating the objectives of two folds; then figure out the approach that makes use of GenCOs' incentives for profit maximization and offers the 'appreciated' price sequence financially stimulating GenCOs to generate the required power trajectory. If such control law is designed, the supply dynamically tracks the demand over a given time horizon and meanwhile each GenCO gains maximal profit for the offered price. Both the ISO and GenCOs achieve their objectives and the win-win collaboration is implemented.

B. Dynamic Model of GenCOs

Denote $x_i^{(k)}$ the generation power of Generator-i (Gi) in PTU-k and assume it keeps constant during PTU-k, the supplied energy is $Tx_i^{(k)}$, the production cost associated to the current generation level is [13], [14], [16]

$$C_{\mathrm{S}}\left(Tx_i^{(k)}\right) = d_i + e_i \cdot Tx_i^{(k)} + \frac{1}{2} f_i \left(Tx_i^{(k)}\right)^2 \quad (1)$$

and the production cost associated to the output variation with respect to the previous PTU [23]

$$C_{\mathrm{V}}\left(T\Delta x_i^{(k)}\right) = \alpha_i \left(Tx_i^{(k)} - Tx_i^{(k-1)}\right)^2 \quad (2)$$

where d_i, e_i, f_i, α_i are constant coefficients of Gi's production.

The net profit of Gi in PTU-k is expressed as its total revenues minus all production costs [23]

$$\pi_i^{(k)} = u_i^{(k-1)} \cdot Tx_i^{(k)} - C_{\mathrm{S}}\left(Tx_i^{(k)}\right) - C_{\mathrm{V}}\left(T\Delta x_i^{(k)}\right). \quad (3)$$

Gi adjusts its output to reach the first-order necessary condition for optimum

$$\frac{\partial \pi_i^{(k)}}{\partial x_i^{(k)}} = \frac{\partial u_i^{(k-1)}}{\partial x_i^{(k)}} Tx_i^{(k)} + Tu_i^{(k-1)} - \left(e_i T + f_i T^2 x_i^{(k)}\right) - 2\alpha_i T^2 \left(x_i^{(k)} - x_i^{(k-1)}\right)\left(1 - \frac{\partial x_i^{(k-1)}}{\partial x_i^{(k)}}\right) = 0. \quad (4)$$

Since the past status/decision won't change with the current decision, i.e., $\partial u_i^{(k-1)}/\partial x_i^{(k)} = \partial x_i^{(k-1)}/\partial x_i^{(k)} = 0$. We rearrange (4) as

$$x_i^{(k)} = \frac{2\alpha_i}{2\alpha_i + f_i} x_i^{(k-1)} + \frac{1/T}{2\alpha_i + f_i} u_i^{(k-1)} - \frac{e_i/T}{2\alpha_i + f_i}. \quad (5)$$

Namely, given the previous state $x_i^{(k-1)}$ and the ISO-proposed price $u_i^{(k-1)}$, Gi could gain highest profit by choosing the output $x_i^{(k)}$, i.e., the incentives for profit maximization are embedded in this price-quantity mapping:

$$x_i^{(k-1)}, u_i^{(k-1)} :\to x_i^{(k)}, i \in \mathcal{G}. \quad (6)$$

The discrete-time state-space equations of n-bus network

$$\boldsymbol{x}^{(k+1)} = \boldsymbol{A}x^{(k)} + \boldsymbol{B}u^{(k)} + \boldsymbol{w} \quad (7)$$

and the output equation

$$y^{(k)} = \boldsymbol{C}x^{(k)} \quad (8)$$

where $\boldsymbol{A}, \boldsymbol{B} \in \mathbb{R}^{n\times n}$ are diagonal matrices, $\boldsymbol{C}^{\mathrm{T}}, \boldsymbol{w} \in \mathbb{R}^n$. $A_{i,i} = (2\alpha_i)/(2\alpha_i + f_i)$, $B_{i,i} = (1/T)/(2\alpha_i + f_i)$, $w_i = -(e_i/T)/(2\alpha_i + f_i)$, $C_i = 1$ iff $i \in \mathcal{G}$; otherwise all the elements equal to 0.

C. Constrained Optimal Tracking Problem Formulation

In the ISO's view, three objectives should be compromised over the preview time horizon.

1) The global power balance

$$\sum_{k=1}^{k_{\mathrm{f}}} \left| \sum_{i\in\mathcal{G}} x_i^{(k)} + \sum_{i\in\mathcal{W}} x_{*i}^{(k)} - \sum_{i\in\mathcal{D}} x_{*i}^{(k)} \right| = \sum_{k=1}^{k_{\mathrm{f}}} \left| y^{(k)} - y_*^{(k)} \right| = 0. \quad (9)$$

2) Lower and more stationary prices for GenCOs

$$\min \sum_{k=1}^{k_{\mathrm{f}}-1} \sum_{i\in\mathcal{G}} \left| u_i^{(k)} \right|. \quad (10)$$

3) Meanwhile the line rating constraints are satisfied

$$\left| \psi_{\mathrm{L}i}^{(k)} \right| \le \bar{\psi}_{\mathrm{L}i} \quad \forall i \in \mathcal{L}, k = 1, \ldots, k_{\mathrm{f}}. \quad (11)$$

Employing the weighted aggregation technique, we integrate the three objectives and derive the linear constrained quadratic optimal tracking problem:

$$\min J_k = \sum_{j=1}^{k_{\mathrm{f}}} \left[\left\| y^{(k+j)} - y_*^{(k+j)} \right\|_Q^2 + \left\| \boldsymbol{\psi}^{(k+j)} \right\|_{\boldsymbol{S}}^2 \right] + \sum_{j=0}^{k_{\mathrm{f}}-1} \left\| \boldsymbol{u}^{(k+j)} \right\|_{\boldsymbol{R}}^2 \quad (12)$$

s.t.

$$\begin{aligned} \boldsymbol{x}^{(k+1)} &= \boldsymbol{A}x^{(k)} + \boldsymbol{B}u^{(k)} + \boldsymbol{w} \\ y^{(k)} &= \boldsymbol{C}x^{(k)} \\ \boldsymbol{\psi}^{(k)} &= \boldsymbol{F} \cdot \left(\boldsymbol{x}^{(k)} - \boldsymbol{x}_*^{(k)}\right) \end{aligned} \quad (13)$$

where $\boldsymbol{S} = \mathrm{diag}\{S_1, \ldots, S_{n_{\mathrm{L}}}\}, \boldsymbol{R} = \mathrm{diag}\{R_1, \ldots, R_n\}$. $Q \ge 0, S_i \ge 0, R_i > 0$ are respectively the weight of global power imbalance, flow through Line-i, price on Bus-i. The values are empirically set. Each element of $\boldsymbol{F} \in \mathbb{R}^{n_{\mathrm{L}}\times n}$ is solely a function of the network's line susceptances.

D. Illustration of Convergence to Market Equilibrium

It should be emphasized that the price-quantity tuple solving problem (12) is the equilibrium rather than the global optimum. Equation (3) indicates that Gi's expected profit π is the concave quadratic function of its generation quantity x. Different prices correspond to different $x-\pi$ curves, and each $x-\pi$ curve has its own optimal solution x_{opt} that achieves the maximal profit π_{opt}. Obviously, the optimality of Gi's response is not absolute but dependent on the proposed price from the ISO. Please refer to the Curve-I, II, and III in Fig. 3, Gi would receive the best profit $\pi_{\mathrm{opt}}^{\mathrm{I}}, \pi_{\mathrm{opt}}^{\mathrm{II}}, \pi_{\mathrm{opt}}^{\mathrm{III}}$ by responding $x_{\mathrm{opt}}^{\mathrm{I}}, x_{\mathrm{opt}}^{\mathrm{II}}, x_{\mathrm{opt}}^{\mathrm{III}}$, if the prices $u^{\mathrm{I}}, u^{\mathrm{II}}, u^{\mathrm{III}}$ are applied, respectively.

The principle of the pricing control is that the ISO is making the best pricing decision (i.e., set the $x-\pi$ curves for GenCOs), taking into account the market requirement and each GenCO's response strategy; and sequentially each GenCO is making the

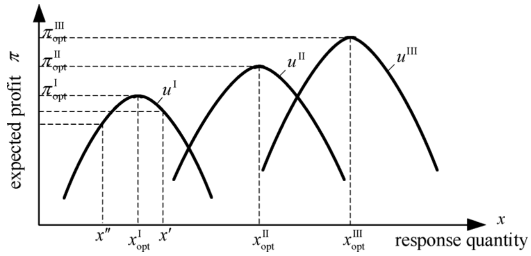

Fig. 3. Optimal strategy of pricing control is the equilibrium.

best response decision (i.e., adjust the output along the specific $x-\pi$ curve), according to the ISO's pricing strategy. In GenCO's view: given the price u^{I}, it would lose some profit if its response deviates from $x^{\mathrm{I}}_{\mathrm{opt}}$; in the ISO's view: given the GenCOs' dynamics, the power imbalance would occur if alternative price is applied, e.g., the ISO sets price from u^{I} to u^{II} will make GenCO respond with $x^{\mathrm{II}}_{\mathrm{opt}}$ rather than $x^{\mathrm{I}}_{\mathrm{opt}}$. Neither the ISO nor a single GenCO has anything to gain by changing only their own strategy unilaterally. It is illustrated that the derived pricing strategy and the resulting response converge to the market equilibrium.

III. Solution of Optimal Pricing Strategy

A. Primer on Information Fusion Estimation (IFE)

Information fusion estimation is the technique widely used in multi-sensor measuring and identification. The key is to comprehensively extract and exploit the information from multiple sensors to improve the reliability and accuracy of state estimation.

Given m sensors for measuring the state $\boldsymbol{\chi} \in \mathbb{R}^n$, each sensor provides a measurement result $\boldsymbol{\zeta}_i$ linearly dependent on the state

$$\boldsymbol{\zeta}_i = \boldsymbol{H}_i \boldsymbol{\chi} + \boldsymbol{\varepsilon}_i, \quad i = 1, 2, \ldots, m \tag{14}$$

where $\boldsymbol{H}_i$ is the information mapping matrix of sensor i and the measurement error $\boldsymbol{\varepsilon}_i$ is white noise with variance $\boldsymbol{\Theta}_i$, i.e.,

$$\mathsf{E}[\boldsymbol{\varepsilon}_i] = \boldsymbol{0}, \quad \mathsf{E}\left[\boldsymbol{\varepsilon}_i \boldsymbol{\varepsilon}_j^{\mathrm{T}}\right] = \begin{cases} \boldsymbol{\Theta}_i, & i = j \\ \boldsymbol{0}, & i \neq j. \end{cases} \tag{15}$$

The task of information fusion estimation is to use the error-interfered-measurement results to optimally estimate the real state $\boldsymbol{\chi}$.

Denote $\mathfrak{F}[\boldsymbol{\zeta}_i]$ the information we can obtain from the measurement result, we have

$$\mathfrak{F}[\boldsymbol{\zeta}_i] = \boldsymbol{\Theta}_i^{-1}. \tag{16}$$

Obviously smaller variance implies less sensor noise, higher reliability measurement and more information could be extracted from $\boldsymbol{\zeta}_i$.

Theorem 1 [34]: Given all measurement results $\{\boldsymbol{\zeta}_i | i = 1, 2, \ldots, m\}$of state $\boldsymbol{\chi}$, which are expressed by (14). If $\sum_{i=1}^{m} \boldsymbol{H}_i^{\mathrm{T}} \boldsymbol{\Theta}_i^{-1} \boldsymbol{H}_i$ is nonsingular, then the optimal information fusion estimation of $\boldsymbol{\chi}$ is

$$\hat{\boldsymbol{\chi}} = \mathfrak{F}^{-1}[\hat{\boldsymbol{\chi}}] \sum_{i=1}^{m} \boldsymbol{H}_i^{\mathrm{T}} \boldsymbol{\Theta}_i^{-1} \boldsymbol{\zeta}_i \tag{17}$$

TABLE I
Comparison of State Estimation and Tracking Control

	Optimal state estimation	Optimal tracking control
unknown, real state	actual variable to be measured	actual supply, price, flow
known data	measurement results from all sensors	predicted demand, wind forecast, line ratings, etc.
accessible, approximated state	estimated variable based on sensor measurements	ideal supply, price, flow based on system requirements
approximation reliability	variance of the measurement error	variance of the tracking error
optimization objective	minimize the cumulative estimation error	minimize the cumulative tracking error

where $\mathfrak{F}[\boldsymbol{\zeta}_i | \hat{\boldsymbol{\chi}}] = \boldsymbol{H}_i^{\mathrm{T}} \mathfrak{F}[\boldsymbol{\zeta}_i] \boldsymbol{H}_i = \boldsymbol{H}_i^{\mathrm{T}} \boldsymbol{\Theta}_i^{-1} \boldsymbol{H}_i$, $\mathfrak{F}[\hat{\boldsymbol{\chi}}] = \sum_{i=1}^{m} \mathfrak{F}[\boldsymbol{\zeta}_i | \hat{\boldsymbol{\chi}}]$.

B. Application of IFE to Optimal Tracking Control

The problems of optimal tracking control and optimal state estimation have essential similarities. As presented in Table I, they both 1) study the real states which are unknown; 2) approximate the real state based on known data; and 3) attempt to make the approximation approach the real state as close as possible. The state estimation could be viewed as a kind of tracking control in which the estimated state optimally tracks the real one; the tracking control could be viewed as a kind of state estimation in which the ideal trajectory optimally estimates the actual one.

Assuming we are at PTU-k, the known information are the current price $\boldsymbol{u}^{(k)}$, current generation $\boldsymbol{x}^{(k)}$ and predicted net demand $\{\boldsymbol{x}_*^{(k+j)}\}_{j=1}^{k_{\mathrm{f}}}$. Besides, we define the costate $\{\hat{\boldsymbol{x}}^{(k+j+1)}\}_{j=1}^{k_{\mathrm{f}}}$ to linkup the estimation and real state:

$$\hat{\boldsymbol{x}}^{(k+j+1)} = \boldsymbol{x}^{(k+j+1)} + \boldsymbol{p}^{(k+j+1)} \quad j = 1, 2, \ldots, k_{\mathrm{f}} \tag{18}$$

where $\boldsymbol{p}^{(k+j+1)}$ is the white noise of variance $(\boldsymbol{P}^{(k+j+1)})^{-1}$. Now we are ready to derive the price sequence $\{\boldsymbol{u}^{(k+j)}\}_{j=1}^{k_{\mathrm{f}}-1}$ by applying the information fusion estimation.

1) There are two information sources concerning $\boldsymbol{u}$

a) expectation for the low and stationary nodal price

$$\boldsymbol{0} = \boldsymbol{u}^{(k+j)} + \boldsymbol{r} = \boldsymbol{I}_n \cdot \boldsymbol{u}^{(k+j)} + \boldsymbol{r} \tag{19}$$

where $\boldsymbol{r}$ is the white noise of variance $\boldsymbol{R}^{-1}$, thus

$$\mathfrak{F}\left[\boldsymbol{0} | \boldsymbol{u}^{(k+j)}\right] = \boldsymbol{I}_n^{\mathrm{T}} \cdot \boldsymbol{R} \cdot \boldsymbol{I}_n = \boldsymbol{R}. \tag{20}$$

b) GenCOs' dynamics described by (7), combining (18)

$$\hat{\boldsymbol{x}}^{(k+j+1)} - \boldsymbol{A} x^{(k+j)} - \boldsymbol{w} = \boldsymbol{B} u^{(k+j)} + \boldsymbol{p}^{(k+j+1)} \tag{21}$$

thus

$$\mathfrak{F}\left[\hat{\boldsymbol{x}}^{(k+j+1)} | \boldsymbol{u}^{(k+j)}\right] = \boldsymbol{B}^{\mathrm{T}} \boldsymbol{P}^{(k+j+1)} \boldsymbol{B}. \tag{22}$$

Theorem 1 gives the optimal information fusion estimation of $\{\boldsymbol{u}^{(k+j)}\}_{j=1}^{k_\mathrm{f}-1}$

$$\begin{aligned}\hat{\boldsymbol{u}}^{(k+j)} &= \left(\mathfrak{F}\left[\boldsymbol{0}|\boldsymbol{u}^{(k+j)}\right] + \mathfrak{F}\left[\hat{\boldsymbol{x}}^{(k+j+1)}|\boldsymbol{u}^{(k+j)}\right]\right)^{-1}\\ &\quad\times\left[\boldsymbol{I}_n^\mathrm{T}\cdot\boldsymbol{R}\cdot\boldsymbol{0} + \boldsymbol{B}^\mathrm{T}\boldsymbol{P}^{(k+j+1)}\right.\\ &\quad\left.\times\left(\hat{\boldsymbol{x}}^{(k+j+1)} - \boldsymbol{A}x^{(k+j)} - \boldsymbol{w}\right)\right]\\ &= \left(\boldsymbol{R} + \boldsymbol{B}^\mathrm{T}\boldsymbol{P}^{(k+j+1)}\boldsymbol{B}\right)^{-1}\boldsymbol{B}^\mathrm{T}\boldsymbol{P}^{(k+j+1)}\\ &\quad\times\left(\hat{\boldsymbol{x}}^{(k+j+1)} - \boldsymbol{A}x^{(k+j)} - \boldsymbol{w}\right).\end{aligned}\tag{23}$$

2) There are three information sources regarding $\boldsymbol{x}$

a) Incentive for the small power unbalance, combining (8)

$$y_*^{(k+j)} = y^{(k+j)} + q = \boldsymbol{C}x^{(k+j)} + q\tag{24}$$

where q is the white noise of variance Q^{-1}, thus

$$\mathfrak{F}\left[y_*^{(k+j)}|\boldsymbol{x}^{(k+j)}\right] = \boldsymbol{C}^\mathrm{T}Q\boldsymbol{C}.\tag{25}$$

b) Combining (7) and (18), yields

$$\hat{\boldsymbol{x}}^{(k+j+1)} - \boldsymbol{w} = \boldsymbol{A}x^{(k+j)} - \boldsymbol{B}r + \boldsymbol{p}^{(k+j+1)}.\tag{26}$$

Thus

$$\begin{aligned}&\mathfrak{F}\left[\hat{\boldsymbol{x}}^{(k+j+1)}|\boldsymbol{x}^{(k+j)}\right]\\ &\quad= \boldsymbol{A}^\mathrm{T}\left[\left(\boldsymbol{P}^{(k+j+1)}\right)^{-1} + \boldsymbol{B}R^{-1}\boldsymbol{B}^\mathrm{T}\right]^{-1}\boldsymbol{A}.\end{aligned}\tag{27}$$

c) The line flow constraints

$$\boldsymbol{0} = \boldsymbol{\psi}^{(k+j)} + \boldsymbol{s}^{(k+j)} = \boldsymbol{F}\left(\boldsymbol{x}^{(k+j)} - \boldsymbol{x}_*^{(k+j)}\right) + \boldsymbol{s}^{(k+j)}\tag{28}$$

where $\boldsymbol{s}^{(k+j)}$ is the white noise of variance $\boldsymbol{S}^{(k+j)}$, thus

$$\mathfrak{F}\left[\boldsymbol{F}x_*^{(k+j)}|\boldsymbol{x}^{(k+j)}\right] = \boldsymbol{F}^\mathrm{T}\boldsymbol{S}^{(k+j)}\boldsymbol{F}.\tag{29}$$

Theorem 1 gives the optimal estimation of $\{\boldsymbol{x}^{(k+j)}\}_{j=1}^{k_\mathrm{f}}$

$$\begin{aligned}&\hat{\boldsymbol{x}}^{(k+j)}\\ &= \left(\boldsymbol{P}^{(k+j)}\right)^{-1}\left\{\boldsymbol{C}^\mathrm{T}Qy_*^{(k+j)} + \boldsymbol{F}^\mathrm{T}\boldsymbol{S}^{(k+j)}\boldsymbol{F}x_*^{(k+j)}\right.\\ &\quad + \boldsymbol{A}^\mathrm{T}\left[(\boldsymbol{P}^{(k+j+1)})^{-1} + \boldsymbol{B}R^{-1}\boldsymbol{B}^\mathrm{T}\right]^{-1}\\ &\quad\left.\times\left(\hat{\boldsymbol{x}}^{(k+j+1)} - \boldsymbol{w}\right)\right\}\end{aligned}\tag{30}$$

$$\begin{aligned}&\boldsymbol{P}^{(k+j)}\\ &= \left\{\mathfrak{F}\left[y_*^{(k+j)}|\boldsymbol{x}^{(k+j)}\right] + \mathfrak{F}\left[\hat{\boldsymbol{x}}^{(k+j+1)}|\boldsymbol{x}^{(k+j)}\right]\right.\\ &\quad\left.+\mathfrak{F}\left[\boldsymbol{F}x_*^{(k+j)}|\boldsymbol{x}^{(k+j)}\right]\right\}\\ &= \boldsymbol{C}^\mathrm{T}Q\boldsymbol{C} + \boldsymbol{A}^\mathrm{T}\left[(\boldsymbol{P}^{(k+j+1)})^{-1} + \boldsymbol{B}R^{-1}\boldsymbol{B}^\mathrm{T}\right]^{-1}\boldsymbol{A}\\ &\quad + \boldsymbol{F}^\mathrm{T}\boldsymbol{S}^{(k+j)}\boldsymbol{F}\\ &\qquad j = k_\mathrm{f}, k_\mathrm{f}-1, \ldots, 1.\end{aligned}\tag{31}$$

The initial conditions for the backward computation are

$$\boldsymbol{P}^{(k+k_\mathrm{f}+1)} = \boldsymbol{C}^\mathrm{T}Q\boldsymbol{C} + \boldsymbol{F}^\mathrm{T}\boldsymbol{S}^{(k+k_\mathrm{f}+1)}\boldsymbol{F}\tag{32}$$

$$\begin{aligned}\hat{\boldsymbol{x}}^{(k+k_\mathrm{f}+1)} &= \left(\boldsymbol{P}^{(k+k_\mathrm{f}+1)}\right)^{-1}\\ &\quad\times\left(\boldsymbol{C}^\mathrm{T}Qy_*^{(k+k_\mathrm{f}+1)} + \boldsymbol{F}^\mathrm{T}\boldsymbol{S}^{(k+k_\mathrm{f}+1)}\boldsymbol{F}x_*^{(k+k_\mathrm{f}+1)}\right).\end{aligned}\tag{33}$$

C. Pseudo Code of IFPC

Set the weight $Q, \boldsymbol{R}, \boldsymbol{S}, nc_{\max}$;

% {Assume the current time is PTU-k}

proc. IFPC

% {Initialization}

$nc = 1$; $rating = 0$;

Read current state $\boldsymbol{x}^{(k)}$;

Read demand $\{\boldsymbol{x}_\mathrm{D}^{(k+j)}\}_{j=1}^{k_\mathrm{f}}$, wind forecast $\{\boldsymbol{x}_\mathrm{W}^{(k+j)}\}_{j=1}^{k_\mathrm{f}}$;

Compute net demand $\{\boldsymbol{x}_*^{(k+j)}\}_{j=1}^{k_\mathrm{f}}$;

Compute $\boldsymbol{P}^{(k+k_\mathrm{f}+1)}, \hat{\boldsymbol{x}}^{(k+k_\mathrm{f}+1)}$ using (32), (33);

While $nc < nc_{\max}$ and $rating == 0$

  % {Backward information fusion estimation for co-state}

    For $j = k_\mathrm{f} : -1 : 1$

      Compute $\boldsymbol{P}^{(k+j)}$, $\hat{\boldsymbol{x}}^{(k+j)}$ using (31), (30);

    EndFor

  % {Forward information fusion estimation for control}

    For $j = 0 : k_\mathrm{f} - 1$

      Compute nodal price $\boldsymbol{u}^{(k+j)}$ using (23);

      Compute $\boldsymbol{x}^{(k+j+1)}$, $y^{(k+j+1)}$, $\boldsymbol{\psi}^{(k+j+1)}$ using (13);

    EndFor

  % {Examine the rating constraints}

    If $\left|\psi_{\mathrm{L}i}^{(k+j)}\right|_{j=1}^{k_\mathrm{f}} > \bar{\psi}_{\mathrm{L}i}$

      % {increase the weight of flow}

      $S_{i,i} \leftarrow \kappa \cdot S_{i,i}$ $(\kappa > 1)$;

    Else

      $rating \leftarrow 1$;

      $S_{i,i} \leftarrow 1/\kappa \cdot S_{i,i}$ $(\kappa > 1)$

    EndIF

    $nc \leftarrow nc + 1$;

EndWhile

Update the actual state $\boldsymbol{x}^{(k+1)}$ and price $\boldsymbol{u}^{(k)}$ of next PTU;

$k \leftarrow k + 1$;

Repeat **proc.IFPC;**

TABLE II
COST PARAMETERS OF GENCOS

GenCO id	1	2	3	4	5	6	7	8	9
generator id (@bus id)	4,6,8, 10,12,15	18,19,24, 25,26,27	31,32,34, 36,40,42	46,49,54, 55,56,59	61,62,65, 66,69,70	72,73,74, 76,77,80	82,85,87, 89,90,91	92,99,100, 103,104,105	107,110,111, 112,113,116
α: \$/MWh^2	0.06	0.06	0.06	0.12	0.12	0.06	0.06	0.12	0.12
f: \$/MWh^2	0.08	0.1	0.1	0.1	0.1	0.15	0.15	0.15	0.15
e: \$/MWh	4	4	6	4	6	4	6	4	6
d: \$	10	10	10	10	10	10	10	10	10

TABLE III
NOMINAL POWER OF LOADS

Load id	1	2	3	4	6	7	11	12	13	14	15	16	17	18	19	20	21	22	23
p_{nom}: MW	510	200	390	300	520	190	700	470	340	140	900	250	110	600	450	180	140	100	70
Load id	27	28	29	31	32	33	34	35	36	39	40	41	42	43	44	45	46	47	48
p_{nom}: MW	620	170	240	430	590	230	590	330	310	270	200	370	370	180	160	530	280	340	200
Load id	49	50	51	52	53	54	55	56	57	58	59	60	62	66	67	70	74	75	76
p_{nom}: MW	870	170	170	180	230	1130	630	840	120	120	2770	780	770	390	280	660	680	470	680
Load id	77	78	79	80	82	83	84	85	86	88	90	92	93	94	95	96	97	98	100
p_{nom}: MW	610	710	390	1300	540	200	110	240	210	480	780	650	120	300	420	380	150	340	370
Load id	101	102	103	104	105	106	107	108	109	110	112	114	115	117	118				
p_{nom}: MW	220	50	230	380	310	430	280	20	80	390	250	80	220	200	330				

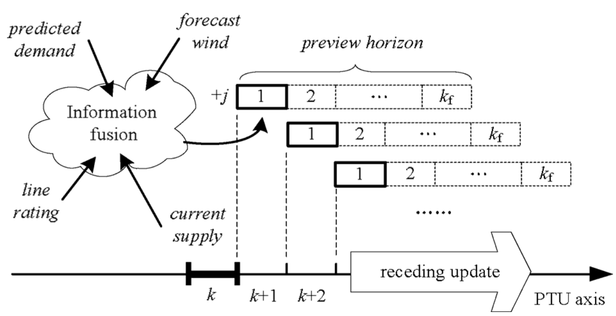

Fig. 4. Principle of information fusion based pricing control (IFPC).

The mechanism of multi-PTU preview and fusion over the receding horizon is illustrated in Fig. 4.

IV. EXPERIMENTAL SETUPS

A. Network

The IEEE 118-bus power system is adopted as the benchmark network for testing the performance of IFPC. As shown in Fig. 5 [35], 54 generators connecting to relevant buses inject power into the network and through 186 lines the user demands are served. The buses, generators and user load demands are denoted by "numbered thick bar", "G" and "solid head arrows", respectively.

B. Data

Consider the large number of generators and for the simplicity of expression and further comparison, we assume that every six generators are managed by one GenCO, e.g., the generators which are installed on the bus B4, B6, B8, B10, B12, B15, belong to GenCO-1. Thus the 54 generators respectively belong to 9 GenCOs. The 6 generators of the same GenCO have the same production cost coefficients, which are listed in Table II. d is the fixed cost, smaller e and f indicate lower cost for given production level, and smaller α implies the less sensitive to output variation. GenCO-1 is the most superior market player whose parameters are not larger than others' while GenCO-9 is the most inferior one whose parameters are not better than others'. In Case 1 and Case 2 of next section, all energy suppliers are thermal generators, i.e., all the 9 GenCOs are price-elastic. In Case 3, GenCO-{4, 7, 9} are price-inelastic wind farms, whose maximal outputs are 476 MW, 490 MW, and 486 MW, respectively.

Table III shows the nominal power of 91 loads, the sum of which is the peak demand (7.336 GW). In Case 3, the peak wind power (1.451 GW) is the total maximal output of GenCO-{4, 7, 9}. Fig. 6 depicts the 72-h trajectory of the normalized predicted demand and forecast wind power. Obviously they have the complementary pattern: the user demand is high during daytime while the wind power peaks at midnight.

C. Performance Index

Indices are defined to evaluate the performance of IFPC in aspects of technical and economical. In the global view of the ISO, *power imbalance* is the degree that the supply deviates from the demand, lower "avg" and "std" imply more accurate and stationary global power match. *Total pay* is the bill that the ISO pays to purchase energy from all GenCOs in the market. *Total cost* reflects the generation efficiency of supplying the given demand.

In the individual view of each GenCO, the *nodal price* is the sole input signal for production decision. Higher price means GenCO could earn more revenue by selling the same volume of energy. *Profit* is GenCO's net income from electricity production. Higher profit indicates the advantages over opponents in the market competition.

V. CASE STUDY

A. Case 1: Concern Neither Wind Penetration Nor Flow Limit

In IFPC, the PTU time T determines the update frequency for the latest information fusion and pricing action; thus might be the key parameter of the performance. In order to focus on the effects of various PTU times, this case assumes that all the

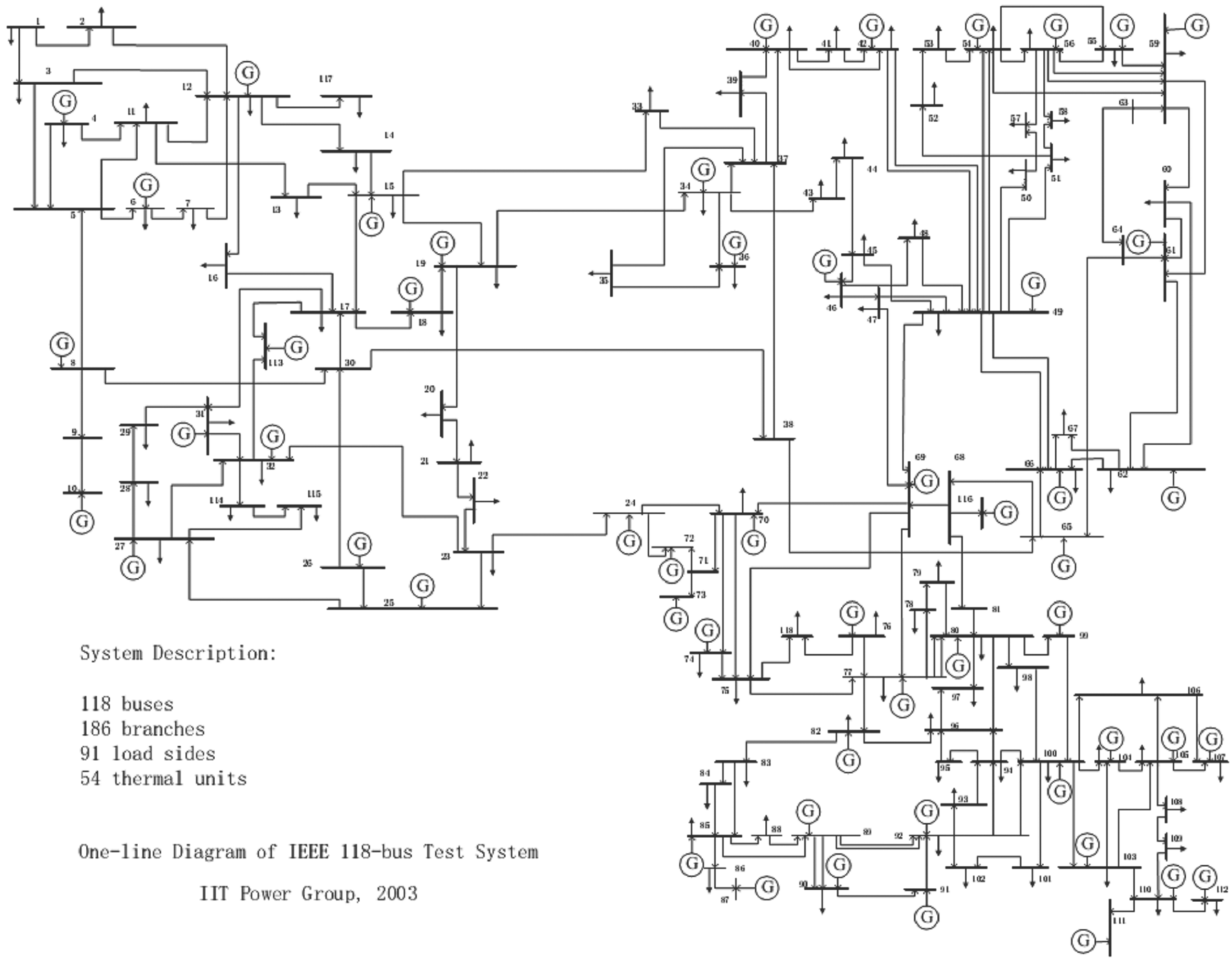

Fig. 5. IEEE 118-bus test network [35].

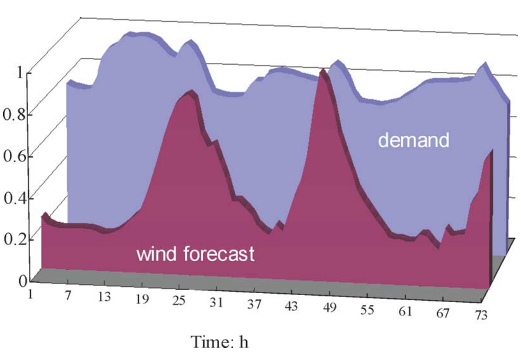

Fig. 6. Profile of 72-h demand and wind forecast (normalized).

9 GenCOs are price-elastic electricity suppliers which possess traditional thermal generators and all the 186 transmission line ratings are large enough. Since neither line congestion nor uncertain power injection is involved, this is a simplified case of the unconstrained linear system operating in the deterministic scenario.

Table IV lists the system macro performances computed at various PTU times. As for the concerns on system safety and reliability, the shorter PTU time brings down both "avg" and "std" of power imbalance. Although the total pay slightly increases from 7.807 M$ to 7.851 M$ $(+0.56\%)$, the total cost is significantly reduced from 4.997 M$ to 2.805 M$ (-44%). In the view of the ISO, reducing the PTU time implies more accurate and stationary power balance and higher macro production efficiency with little total pay increment.

TABLE IV
IMPACT OF PTU TIME ON SYSTEM MACRO PERFORMANCE

PTU (h)	Power imbalance (%) avg (10^{-4})	Power imbalance (%) std (10^{-6})	Total pay (M$)	Total cost (M$)
1	1.549	9.427	**7.807**	4.997
1/2	1.487	4.113	7.818	3.587
1/4	1.457	3.853	7.836	2.961
1/6	**1.453**	**3.793**	7.851	**2.805**

In the individual view of GenCOs, they also could benefit from adopting shorter PTUs. As illustrated in Fig. 7, all the profits monotonously increase as the PTU time varies from 1 h to 1/6 h. However the profit rising rates are quite different: significance of GenCO-$\{4, 5\}$ versus slightness of GenCO-$\{6, 7\}$. Besides the top 5 profit winners also change with PTU time: they are GenCO-$\{1, 2, 3, 6, 7\}$ at $T = 1$ h and GenCO-$\{1, 2, 3, 4, 5\}$ at $T \leq 1/4$ h.

These phenomena could be interpreted by the interactions of GenCO cost parameters and PTU. When PTU time is long (e.g., $T = 1$ h), the information fusion is conducted every 1

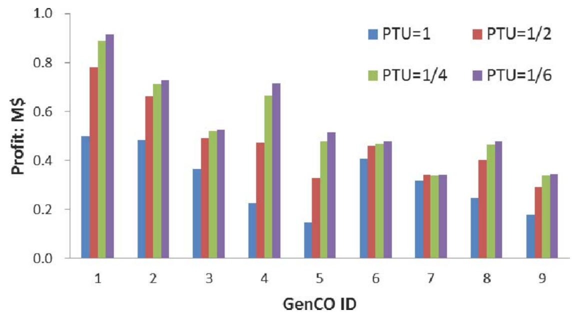

Fig. 7. Total profit of 9 GenCOs in 72 h.

h, the input reference (price) variation with respect to the previous one could be very large, thus GenCOs' output (generation quantity) also changes significantly, $C_{\rm V}$ dominates the total cost. So GenCOs of smaller α could save more cost and belong to the superior group in competition. In Fig. 7, GenCO-$\{1, 2, 3, 6, 7\}$ are featured by having $\alpha = 0.06$. Along with the decrement of PTU time (e.g., $T \leq 1/4$ h), the information fusion is updated more frequently and the input as well as output variation is more smoothened. The weight of $C_{\rm V}$ in the total cost is greatly reduced. Since smaller f implies more cost savings even at large generation quantities, GenCOs of smaller f takes the advantages. In Fig. 7, GenCO-$\{1, 2, 3, 4, 5\}$ are classified by having $f \leq 0.1$.

Notice that GenCO-$\{4, 5\}$ have large α but small f. With the shortening of PTU time, they are "promoted" from the inferior group to superior one and their profits increase significantly. On the contrary, GenCO-$\{6, 7\}$ have small α but large f, they lose the relative advantages when PTU time becomes shorter. Therefore their profits increase slightly.

Since the system reliability, production efficiency, individual profit are all improved through applying shorter PTU time, (the only loss might be the slightly higher total pay for buying the energy), we believe that shorter PTU time is more appreciated by both the market operator and the energy suppliers, from the aspect of technology to economy. However consider the real generators' inertia and response time in practice, it is impossible to implement too short PTUs. In the following tests, the PTU time is set as $T = 1/4$ h, i.e., the information fusion for pricing control is conducted every 15 min.

B. Case 2: Concern None Wind Penetration But Flow Limit

In this case the line ratings are taken into account and IFPC is evaluated by operating the flow constrained network. The tests are designed for answering two questions: firstly whether IFPC is flexible enough to handling various flow limits; secondly whether IFPC is robust enough to maintain the performance in the congested network.

The test of Case 1 reveals that L54 (B30→B38) and L96 (B38→B65) are the top two 'busy' lines, which transmit the highest power flow. Without the loss of generality, we consider four sets of flow rating on L54 and L96 in the following test: 1) $\bar{\psi}_{\rm L54} = \bar{\psi}_{\rm L96} = \infty$, i.e., no flow constraint; 2) $\bar{\psi}_{\rm L54} = 400, \bar{\psi}_{\rm L96} = 350$; 3) $\bar{\psi}_{\rm L54} = 380, \bar{\psi}_{\rm L96} = 300$; 4) $\bar{\psi}_{\rm L54} = 200, \bar{\psi}_{\rm L96} = 150$. Fig. 8 depicts 72-h flow trajectories of L54 and L96 and Table V presents the system macro

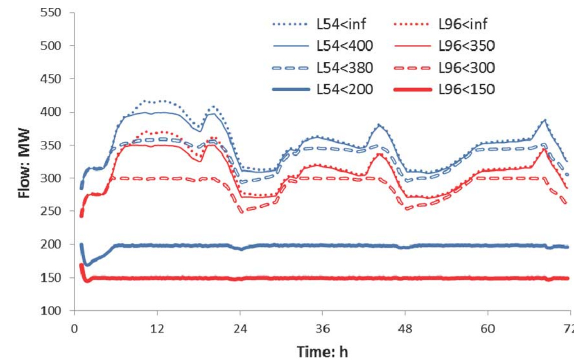

Fig. 8. Flow chart of L54 and L96 under line rating 1)–4).

TABLE V
IMPACT OF LINE RATINGS ON SYSTEM MACRO PERFORMANCE

Line rating (MW)	Power imbalance (%)		Total pay (M$)	Total cost (M$)
L54, L96	avg (10^{-4})	std (10^{-6})		
inf, inf	**1.457**	3.853	**7.836**	**2.961**
400, 350	1.459	3.707	7.837	2.961
380, 300	1.471	**3.186**	7.840	2.963
200, 150	1.539	3.334	7.889	2.982

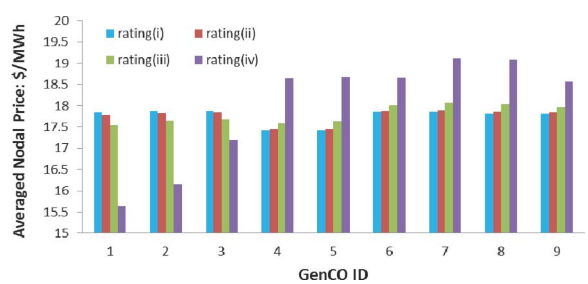

Fig. 9. Average nodal price for GenCOs under line ratings 1)–4).

performance. It could be observed that in rating 1) the flows are almost synchronous to the system demand since no line congestion presents and all GenCOs could output freely to achieve the optimum.

When rating 2) is applied, the flow trajectories of L54 and L96 almost overlap those under rating 1) during most period in 72 h. The two lines are congested only when high demand presents (approximately from 9 h to 15 h of the first day) and the amplitude is accurately clamped at 400 MW and 350 MW, respectively. Since the flows are slightly different from those of rating 1), all the performances in Table V just degrade slightly.

As the line ratings are set even lower. The congestion time of L54, L96 become longer. The congestion always presents on L96 if $\bar{\psi}_{\rm L96} = 150$ is applied. Meanwhile the performances slightly decline: the total pay and total cost respectively increase by $+0.69\%$ and $+0.74\%$, as compared to the unconstrained case.

Although specific lines are congested, IFPC still could ensure the global power balance $(\text{error} < 0.02\%)$ by generation redispatch and flow redistribution. Notice that L54 (B30→B38) and L96 (B38→B65) are the backbones connecting the western and eastern areas of the network in Fig. 5. The test of Case 1 shows the flows through L54 and L96 are of high positive values. It implies that large volume of energy generated in the western area

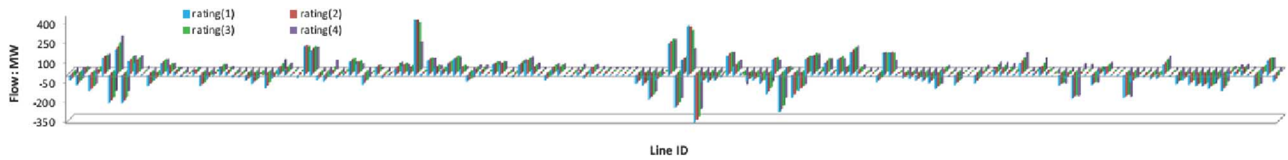

Fig. 10. Flow distribution at peak demand PTU under line ratings 1)–4).

is transmitted to supply the load in the eastern area. Applying flow constraints on L54 and L96 is equivalent to suppress the output of GenCOs in the western area. Fig. 9 shows that the averaged nodal prices for GenCO-{1, 2} are significantly reduced to discourage their production because they are located in the western area; GenCO-3 is also affected because 2 generators of it (G31, G32) are installed in the western area. On the contrary, GenCO-{4, 5, 6, 7, 8, 9}, which are located in the eastern area, are all proposed higher price and greatly encouraged to increase theirs supplies to meet the demand in the eastern area.

The aforementioned tests verify that IFPC is capable of dealing with various flow constraints. It is also revealed that the solution quantity is inferior to that of unconstrained case, and tighter constraints result in poorer performance. The reason is that lower ratings imply the easier and longer congestion. Once congestion occurs, extra expenses have to be paid to call for other GenCOs increase production or transmit power through other lines, which would result in the inferior solution. As specific lines are congested and the generation schedules are modified, the power flows are rerouted and redistributed among the lines of the network, which are depicted in Fig. 10.

C. Case 3: Concern Both Wind Penetration and Flow Limit

In this case we place wind power generation companies (W-GenCOs) into the network and validate IFPC in the scenario of uncertainty. Let GenCO-{4, 7, 9} be W-GenCOs, whose generation profiles are solely dependent of the real time natural wind. We do not apply IFPC on W-GenCOs so as to make best use of the renewable energy. Nevertheless the global power balance and line ratings still should be guaranteed.

The wind forecast of the coming 2 hours is updated at every PTU. Since the farther future causes less reliable forecast, the relative forecast error is simulated as

$$\varepsilon_{\mathrm{W}i}^{(k)} = \mathrm{PTU} \cdot \beta(k-1) \cdot (\mathrm{rand} - 0.5)$$
$$k = 1, \ldots, k_{\mathrm{f}} + 1 \quad (34)$$

where "rand" is a random number uniformly distributed over [0, 1], and the scalar β determines the maximal forecast error in the coming 2 h. Given $T = 1/4$ (i.e., $k_{\mathrm{f}} = 8$) and $\beta = 0.1$, the real wind may deviate from the forecast $\pm 10\%$ in maximum.

The IFPC is tested under 4 different forecast error settings and the line ratings are also taken in consideration. The computational results of Table VI indicate that the forecast error has little impact on IFPC's performance, no matter the line is congested or not. For instance, as the forecast error varies from 0 to 20%, the total pay increases by $+0.094\%$ (from 8.552 M$ to 8.560 M$) given $\bar{\psi}_{\mathrm{L54}} = \infty$ and the total cost is almost invariant (at 2.853 M$) given $\bar{\psi}_{\mathrm{L54}} = 350$ MW. However the line ratings have higher impact on IFPC's performance. For instance given zero forecast error, the total pay increases by $+3.1\%$ (from 8.552 M$ to 8.816 M$) if constrained by $\bar{\psi}_{\mathrm{L54}} = 350$ MW, and given 20% forecast error, the total cost increases by $+2.3\%$ (from 2.789 M$ to 2.853 M$).

TABLE VI
IMPACT OF WIND FORECAST ERROR ON SYSTEM MACRO PERFORMANCE

L54 rating (MW)	Forecast error (%)	Power imbalance (%)		Total pay (M$)	Total cost (M$)
		avg(10^{-4})	std(10^{-5})		
inf	0	**1.933**	**5.956**	**8.552**	**2.786**
	5	1.932	6.020	8.553	2.786
	10	1.932	6.400	8.557	2.787
	20	1.933	8.063	8.560	2.789
350	0	**2.170**	**3.805**	**8.816**	**2.853**
	5	2.171	4.227	8.817	2.853
	10	2.171	4.983	8.818	2.853
	20	2.173	6.939	8.820	2.853

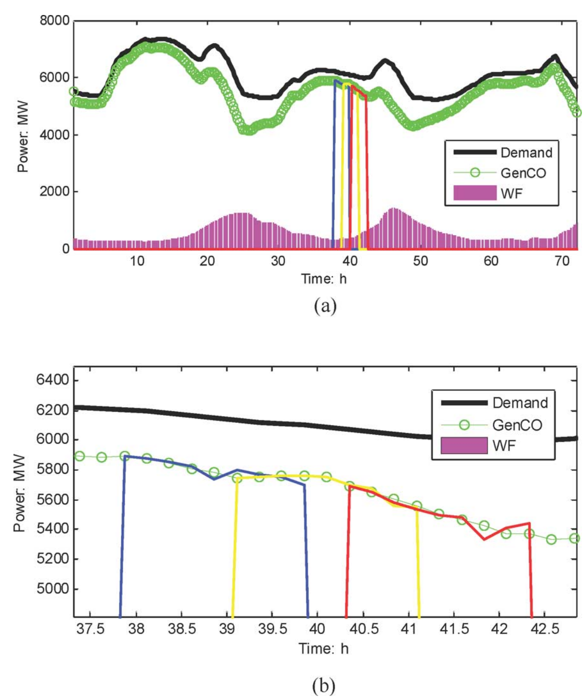

Fig. 11. Performance of IFPC under ±10% wind forecast error. (a) Global view. (b) Local view.

Fig. 11(a) depicts IFPC's performance simulated at $\beta = 0.1, \bar{\psi}_{\mathrm{L54}} = 350$ MW. The total actual supply of all GenCOs (circled green line) and W-GenCOs (pink bar) dynamically tracks the system demand (dashed black line). In order to demonstrate the mechanism of receding preview horizon over the coming 2 h, the scheduled generation profile of GenCOs at PTU-150, 155, and 160 are emphasized with thick lines of blue, yellow, and red, respectively. The "zoom in" local view is shown in Fig. 11(b) and we could obviously observe that the

TABLE VII
PERFORMANCE COMPARISON OF NPD AND IFPC

Test	approach	Power imbalance (%)		Total pay	Total cost	1# PC (desktop) compute time (ms)		2# PC (laptop) compute time (ms)	
		avg(10^{-4})	std(10^{-6})	(M$)	(M$)	avg	max	avg	max
A	NPD	3.330	10.80	7.841	2.963	**2.14**	**11.12**	**13.29**	**41.30**
	IFPC	**1.457**	**3.853**	**7.836**	**2.961**	10.53	20.02	114.21	255.33
B	NPD	3.650	40.33	8.842	2.854	**7.32**	**26.52**	**108.04**	**247.58**
	IFPC	**2.171**	**4.983**	**8.818**	**2.853**	46.97	968.19	251.07	6085.23

schedules are dynamically updated based on the information fusion of the most recent wind forecast, etc.

The test results of this case indicate that IFPC functions well under the wind forecast error varies from zero to 20%. The robustness of IFPC against uncertainties is verified. Since we define the "net demand" $\boldsymbol{x}_*$ to integrate the effects of wind power injection $\boldsymbol{x}_{\mathrm{W}}$ and user demand $\boldsymbol{x}_{\mathrm{D}}$, this case could be easily extended to dealing with the problems which take account for the demand side uncertainty, elasticity, etc.

VI. COMPARATIVE DISCUSSION

The IFPC presented in this paper is mainly inspired by the idea of "negotiated predictive dispatch" (NPD) proposed by [23]. Although they both compromise the ISO's global considerations with the GenCOs' individual profit and utilize the receding preview horizon to incorporate the most recently updated information, the IFPC approach identifies itself from the NPD from the model formulation to the solving technique.

In the optimization model of NPD, the objective is to obtain the price sequence which minimizes the total production cost. The solution is rigorously subject to the constraints of global power balance, line ratings, etc. The nodal prices for each GenCO are initialized at the same value and would be repeatedly modified by the "negotiation" procedure until the feasible dispatch is found.

The IFPC of our proposal aims to minimize the cumulative deviation of power imbalance, nodal price and line flows. The solution is subject to GenCOs' incentives for profit maximization and flow limits. At every PTU, the nodal prices and costates for each GenCO are computed backward by fusing the latest available information. The weight of line flow in the objective function would be repeatedly modified until the line rating constraints are satisfied.

We compare and evaluate the two approaches' performance by applying two tests. In Test A, all the 9 GenCOs operate traditional thermal generators and all line ratings are large enough. Thus the two approaches may have the opportunity to exhibit their capabilities and to achieve the best performance. In Test B, GenCO-{4, 7, 9} are wind farms running wind turbines, L54' rating is limited at 350 MW, and the wind forecast error is $\pm 10\%$. The pricing law is derived by solving the constrained optimization problem with random interferences, i.e., the fluctuating wind. Both programs are coded in Matlab 7 and run on two computation platforms:

1# PC (desktop) that is equipped with i3-2130 CPU@3.40 GHz and 4 GB RAM.

2# PC (laptop) that is equipped with E-450 APU@1.65 GHz and 2 GB RAM.

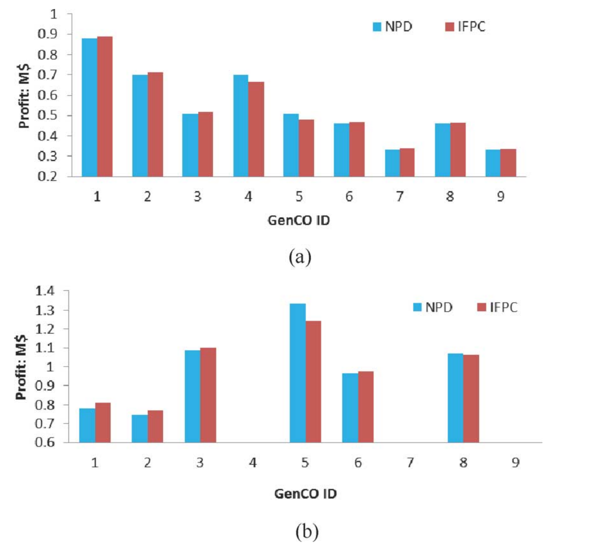

Fig. 12. Comparison of GenCOs' profit by adopting NPD/IFPC. (a) Test A: No line rating, no wind penetration. (b) Test B: concerning L54 rating and GenCO-{4, 7, 9} are W-GenCOs.

In the global view of the ISO, Table VII indicates that IFPC outperforms NPD on most indexes such as the "avg" and "std" power imbalance, total pay and total cost. But NPD could elapse 1/5–1/6 shorter computing time to obtain the solution. The main reason is that the information fusion procedure requires heavy computations on the multiplication and inversion of large scale matrices.

Consider the individual interest of GenCO. Fig. 12 presents each GenCO's profit in the two tests. In Test A, most GenCOs except GenCO-{4, 5} could gain a little higher profit by applying IFPC. And in Test B, GenCO-{1, 2, 3, 6} receive more profit but GenCO-{5, 8} lose profit if IFPC is adopted. IFPC takes slight advantages over NPD. The nodal price trajectories of Test B are shown in Fig. 13, it is observed that the two prices have similar waveforms and they both separate when line congestion presents, however the price divergence among different buses of IFPC is apparently larger.

To summarize, IFPC is inspired from the idea of NPD and they both employ the receding preview horizon technique to incorporate the latest data. Due to the application of comprehensive information fusion, IFPC outperforms NPD on the power imbalance level and stationarity, total pay, total cost, and most GenCOs' individual profit, especially in uncongested networks. NPD is far superior to IFPC on the computing time. Nevertheless IFPC still could obtain the pricing law within 0.97 s (on desktop PC) and 6.1 s (on laptop PC) even at the worst case in the test. Since this computing time is neglectable as compared to the duration of the whole PTU (15 min), we believe that IFPC

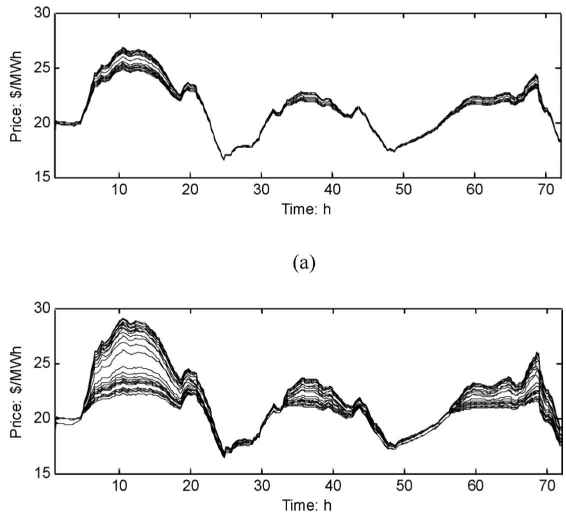

(a)

(b)

Fig. 13. Comparison of price by adopting NPD/IFPC in Test B. (a) Nodal price of NPD. (b) Nodal price of IFPC.

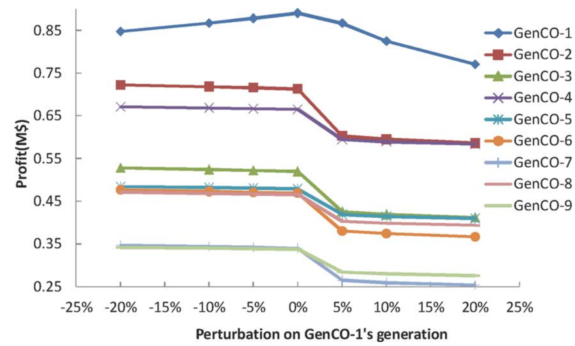

Fig. 14. Impact of GenCO-1's irrational behavior: deviating from optimal generation quantity.

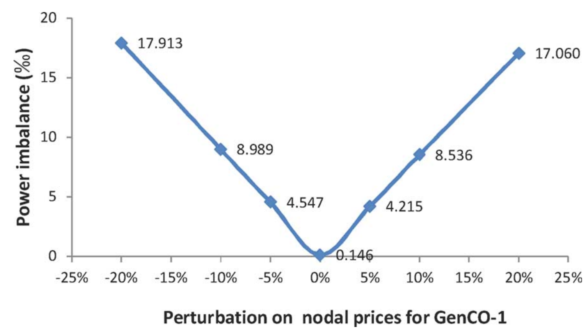

Fig. 15. Impact of the ISO's irrational behavior: deviating from optimal nodal prices.

satisfies the "real time" requirement of pricing control, and IFPC is more appreciated by the ISO and most GenCOs due to the improved global efficiency and expanded individual profits.

VII. Complex Behaviors Exploration

A. Irrational Behaviors and Market Equilibrium

In Section II-D, we have theoretically interpreted that the obtained $u{-}x$ tuple is the market equilibrium by employing the static game theoretic approach. In this subsection, we further examine that the optimal strategy is the market equilibrium in the dynamic market environment with experimental results.

Test A verifies the optimality of GenCO's response strategy. Without loss of generality, it is assumed that only GenCO-1 perturbs its output from optimum by $\pm 5\%$, $\pm 10\%$, $\pm 20\%$, all other GenCOs and the ISO follow the optimal strategies. The simulation settings are the same as those in Section V-A. The impact of GenCO-1's response perturbation on the individual profit of each GenCO is depicted in Fig. 14. It is observed that GenCO-1 would lose profit if it deviated from the optimal response. And larger deviation results in larger profit loss, no matter the deviation are positive or negative. However the profit of any other GenCO is inversely related to GenCO-1's response perturbation. The reason is that if GenCO-1 unilaterally decreased its generation (negative perturbation), other GenCOs would be proposed higher prices to encourage production thus they receive more profit; if GenCO-1 unilaterally increased its generation (positive perturbation), other GenCOs would be proposed lower prices to discourage production thus they receive fewer profit. As the rational market player, each GenCO is willing to adopt the obtained response strategy as optimal.

Test B verifies the optimality of the ISO's pricing strategy. Without loss of generality, it is assumed that the ISO only perturbs the nodal prices for GenCO-1 from optimum by $\pm 5\%, \pm 10\%, \pm 20\%$, all GenCOs follow the optimal response strategies of their own. The impact of the ISO's price perturbation on the global power imbalance is depicted in Fig. 15. It is observed that the global power imbalance would dramatically increase as some nodal prices deviated from optima. As the rational market coordinator, the ISO is willing to apply the obtained pricing strategy as optimal.

B. GenCO's Speculation Behaviors

The principle of IFPC is that the ISO and GenCOs interact via proposing and responding to the nodal price. The ISO decides the pricing law based on its "believed" values of GenCOs' dynamics, i.e., $\hat{e}, \hat{f}, \hat{\alpha}$ [see (23) and (30)], and GenCOs decides the output profile based on the actual values of their own dynamics, i.e., e, f, α [see (5)]. In preceding sections, it is assumed that the "believed" values are identical to the actual counterparts. However the discrepancy unavoidably presents when IFPC is implemented in the real electricity market. If the "believed" values are estimated from historic data, estimation error may occur; if the "believed" values are obtained by GenCOs' bidding, GenCOs may exhibit speculation behaviors so as to gain extra profits.

In the following test, it is assumed that only GenCO-3 deceives the ISO by overbidding/underbidding its production coefficients. We focus on the impact of speculation behavior on the averaged power imbalance and GenCO-3's profit. In Fig. 16, the x-axis "deceiving ratio" is the ratio of the "believed value" versus the "actual value", e.g., $\hat{e}/e$, etc.; the y-axis is the normalized power imbalance or GenCO-3's profit over that under the ideal condition, i.e., $\hat{e} = e$, etc.

Fig. 16(a) shows that any deceiving ratio varying from -30% to $+30\%$ would downgrade the global power balance. The error of f has the greatest impact and the error of α has little impact. However the IFPC is robust against the model variation, since

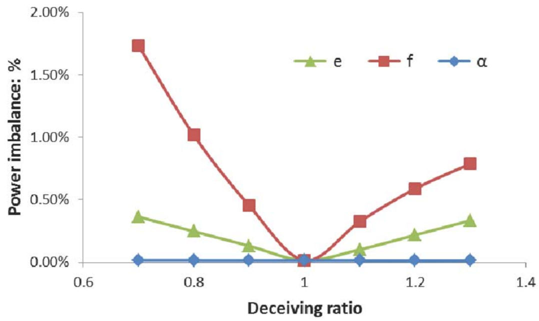

(a)

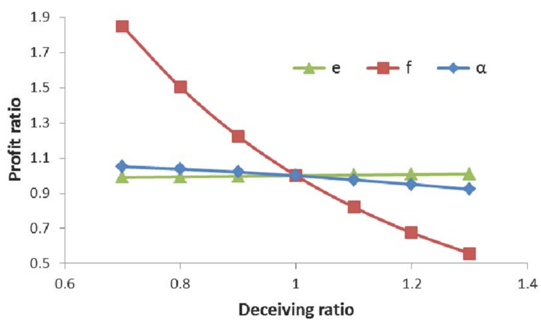

(b)

Fig. 16. Impact of GenCO's speculation behaviors on IFPC's performance. (a) Global power imbalance. (b) Individual profit.

the power imbalance is kept within 1.8% even the parameter is misidentified by 30%. Fig. 16(b) demonstrates that underbidding of f, α and overbidding of e could bring in more profit. The error of f also has the greatest impact and the error of e has little impact. Notice that GenCO-3 nearly doubles its profit by successfully making the ISO believe its f is 30% lower than the actual value.

Simulation results indicate that f is the critical parameter in IFPC. In the real electricity market adopting IFPC, the ISO should figure out how to obtain the accurate f to ensure the global performance and GenCOs would attempt to deceive the ISO that they have lower f than the actuality.

VIII. Conclusion and Perspective

This paper proposes the IFPC mechanism to financially regulate the GenCOs' generation profiles in the liberalized wholesale electricity market. Through compromising the information of demand, supply, wind forecast and transmission limits, the ISO sets the proper nodal prices by making use of GenCOs' incentives for profit maximization; GenCOs response to the prices with the proper generation quantity so as to make maximal profit. Thus the market is described by a state feedback control system, in which the ISO and GenCOs are respectively the controller and plant. And the control system is formulated as a quadratic optimal tracking problem subject to GenCOs' dynamics and line rating constraints. This pricing law is repeatedly computed and updated by applying the technique of information fusion estimation over the receding preview horizon. Numerical results verifies that the IFPC strategy is effective on cases of both deterministic and uncertain, and capable of dealing with various line flow constraints as well as incorporating the wind power fluctuations. The IFPC is also compared to the method of NPD by which the original idea of IFPC is inspired. IFPC exhibits slightly better performance than NPD but requires longer computing time. The irrational behavior analysis proves that the obtained price-response tuple is the market equilibrium, thus neither GenCO nor ISO would unilaterally make deviation. The speculation behavior analysis reveals that the global performance of IFPC would decline due to the parameter misidentification, and GenCOs could gain extra profit by deceive the ISO with lower parameters, especially the quadratic coefficient f. The current work of our research is to 1) further develop the capability of IFPC on the cases of demand-side response and 2) further investigate the complex and diversified behaviors of GenCOs when adopting IFPC in the real electricity market. With the increasing popularization of the smart grid, IFPC is practically enabled by ICT and its potentials in the next generation of power system would be thoroughly recognized and exploited.

References

[1] F. F. Wu, K. Moslehi, and A. Bose, "Power system control centers: Past, present, and future," *Proc. IEEE*, vol. 93, no. 11, pp. 1890–1908, Nov. 2005.

[2] Z. Fan, T. Horger, and J. Bastian, "Current and emerging challenges in PJM energy market," in *Proc. Transmission and Distribution Conf. Expo. (PES)*, 2010, pp. 1–7.

[3] F. C. Schweppe, R. D. Tabors, J. L. Kirtley, H. R. Outhred, F. H. Pickel, and A. J. Cox, "Homeostatic utility control," *IEEE Trans. Power App. Syst.*, vol. PAS-99, no. 3, pp. 1151–1163, 1980.

[4] G. Li, J. Shi, and X. Qu, "Modeling methods for GenCo bidding strategy optimization in the liberalized electricity spot market—A state-of-the-art review," *Energy*, vol. 36, no. 8, pp. 4686–4700, 2011.

[5] L. Wu and M. Shahidehpour, "A hybrid model for day-ahead price forecasting," *IEEE Trans. Power Syst.*, vol. 25, no. 3, pp. 1519–1530, Aug. 2010.

[6] M. H. Albadi and E. F. El-Saadany, "A summary of demand response in electricity markets," *Elect. Power Syst. Res.*, vol. 78, no. 11, pp. 1989–1996, 2008.

[7] J. Kim and A. Shcherbakova, "Common failures of demand response," *Energy*, vol. 36, no. 2, pp. 873–880, 2011.

[8] I. Lampropoulos, N. Baghină, W. L. Kling, and P. F. Ribeiro, "A predictive control scheme for real-time demand response applications," *IEEE Trans. Smart Grid*, to be published.

[9] T. G. Hovgaard, S. Boyd, L. F. Larsen, and J. B. J. O. Rgensen, "Nonconvex model predictive control for commercial refrigeration," *Int. Journal Control*, pp. 1–18, 2013, no. ahead-of-print.

[10] M. P. Moghaddam, A. Abdollahi, and M. Rashidinejad, "Flexible demand response programs modeling in competitive electricity markets," *Appl. Energy*, vol. 88, no. 9, pp. 3257–3269, 2011.

[11] J. M. Lujano-Rojas, C. A. U. Monteiro, R. Dufo-López, and J. E. L. Bernal-Agustín, "Optimum residential load management strategy for real time pricing (RTP) demand response programs," *Energy Policy*, vol. 45, pp. 671–679, 2012.

[12] A. D. Yucekaya, J. Valenzuela, and G. Dozier, "Strategic bidding in electricity markets using particle swarm optimization," *Elect. Power Syst. Res.*, vol. 79, no. 2, pp. 335–345, 2009.

[13] A. Syothert and I. MacLeod, "Competitive bidding as a control problem," *IEEE Trans. Power Syst.*, vol. 15, no. 1, pp. 88–94, Feb. 2000.

[14] G. Gutierrez-Alcaraz and G. B. Sheble, "Generation companies decision-making modeling by linear control theory," *Elect. Power Syst. Res.*, vol. 80, no. 7, pp. 815–827, 2010.

[15] G. Gutierrez-Alcaraz and R. A. Ramos-Trujillo, "GenCos' strategic behavior monitoring on auction bidding based on state variables formulation," in *Proc. Int. Conf. Power System Technology (POWERCON)*, 2010, pp. 1–6.

[16] Y. Liu and F. F. Wu, "Generator bidding in oligopolistic electricity markets using optimal control: Fundamentals and application," *IEEE Trans. Power Syst.*, vol. 21, no. 3, pp. 1050–1061, Aug. 2006.

[17] M. Roozbehani, M. A. Dahleh, and S. K. Mitter, "Volatility of power grids under real-time pricing," *IEEE Trans. Power Syst.*, vol. 27, no. 4, pp. 1926–1940, Nov. 2012.
[18] S. Mei and J. Zhu, "Mathematical and control scientific issues of smart grid and its prospects," *Acta Automatica Sinica*, vol. 39, no. 2, pp. 119–131, 2013.
[19] G. Li and J. Shi, "Agent-based modeling for trading wind power with uncertainty in the day-ahead wholesale electricity markets of single-sided auctions," *Appl. Energy*, vol. 99, no. 11, pp. 13–22, 2012.
[20] P. Zhang, F. Li, and N. Bhatt, "Next-generation monitoring, analysis, and control for the future smart control center," *IEEE Trans. Smart Grid*, vol. 1, no. 2, pp. 186–192, 2010.
[21] M. Kolhe, "Smart grid: Charting a new energy future: Research, development and demonstration," *Electricity J.*, vol. 25, no. 2, pp. 88–93, 2012.
[22] M. Roozbehani, M. Dahleh, and S. Mitter, "On the stability of wholesale electricity markets under real-time pricing," in *Proc. 49th IEEE Conf. Decision and Control (CDC)*, 2010, pp. 1911–1918.
[23] J. Warrington, S. Mariethoz, and M. Morari, "Negotiated predictive dispatch: Receding horizon nodal electricity pricing for wind integration," in *Proc. 8th Int. Conf. European Energy Market (EEM)*, 2011, pp. 407–412.
[24] J. Warrington, P. Goulart, S. Mariethoz, and M. Morari, "A market mechanism for solving multi-period optimal power flow exactly on AC networks with mixed participants," in *Proc. American Control Conf. (ACC), 2012*, 2012, pp. 3101–3107.
[25] A. Virag, A. Jokic, I. Lampropoulos, R. M. Hermans, and P. P. J. van den Bosch, "An alternative approach for real-time balancing of electrical power systems," in *Proc. 9th Int. Conf. European Energy Market (EEM)*, 2012, pp. 1–7.
[26] P. R. MacGregor and H. B. Puttgen, "A spot price based control mechanism for electric utility systems with small power producing facilities," *IEEE Trans. Power Syst.*, vol. 6, no. 2, pp. 683–690, May 1991.
[27] S. Borenstein, M. Jaske, and A. Rosenfeld, "Dynamic pricing, advanced metering, and demand response in electricity markets," in *Center for the Study of Energy Markets*, 2002, UC Berkeley.
[28] K. Xie, Y. H. Song, J. Stonham, E. Yu, and G. Liu, "Decomposition model and interior point methods for optimal spot pricing of electricity in deregulation environments," *IEEE Trans. Power Syst.*, vol. 15, no. 1, pp. 39–50, Feb. 2000.
[29] A. Jokic, M. Lazar, and P. Van den Bosch, "Real-time control of power systems using nodal prices," *Int. J. Elect. Power Energy Syst.*, vol. 31, no. 9, pp. 522–530, 2009.
[30] R. M. Hermans, P. Van den Bosch, A. Jokic, P. Giesbertz, P. Boonekamp, and A. Virag, "Congestion management in the deregulated electricity market: An assessment of locational pricing, redispatch and regulation," in *Proc. 8th Int. Conf. European Energy Market (EEM)*, 2011, pp. 8–13.
[31] R. M. Hermans *et al.*, "Assessment of non-centralised model predictive control techniques for electrical power networks," *Int. J. Control*, vol. 85, no. 8, pp. 1162–1177, 2012.
[32] E-Price Project [Online]. Available: http://www.e-price-project.eu/website/TLL/eprice.php
[33] P. Driessen, R. M. Hermans, and P. van den Bosch, "Distributed economic model predictive control of networks in competitive environments," in *Proc. IEEE 51st Annual Conf. Decision and Control (CDC)*, 2012, pp. 266–271.
[34] Z. Zhen, Z. Wang, and D. Wang, "Information fusion estimation based preview control for discrete linear system," *Acta Automatica Sinica*, vol. 36, no. 2, pp. 347–352, 2010.
[35] IEEE-118-Bus Test System [Online]. Available: http://motor.ece.iit.edu/data/IEEE118bus_inf

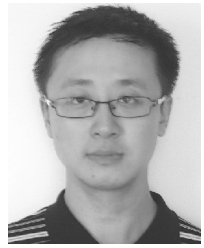

Zhi-Yu Xu received the B.Eng. and Ph.D. degrees in control science and engineering from Tongji University, Shanghai, China, in 2004 and 2010, respectively.

His postdoctoral research was on computer science from 2010 to 2012. In 2006 he was granted 1st Sino-French exchange scholarship and participated in the joint research project of INRIA and ENSMP in France for one year. He is currently an Assistant Professor with Tongji University and the head of Joint-lab of Tongji University and Schneider Electric. His research interests include electricity market modeling and analysis, optimal control theory and application on real-time pricing.

Dr. Xu has been a member of the Chinese Association of System Simulation since 2008. He was the chair on the "nonlinear system" session of 24th Chinese Control and Decision Conference (CCDC) and a peer reviewer of IEEE Transactions, 9th Asia Control Conference (ASCC) and 32nd Chinese Control Conference (CCC).

Wei-Sheng Xu received the B.Eng., M.S., and Ph.D. degrees from Tongji University, Shanghai, China, in 1989, 1992 and 1996, respectively.

Since 2007, he has been the director of the Department of Control Science and Engineering of Tongji University. He was a visiting scholar at the University of Illinois at Urbana-Champaign (UIUC) in 2007. His research interests cover intelligent control theory and applications, energy management and informatization in smart grid, etc.

Prof. Xu is currently a member of the Chinese Association of Automation and the invited chair of Sino-German School of Tongji University.

Wei-Hui Shao received the B.Eng. degree from Tongji University, Shanghai, China, in 2011, where he is currently pursuing the Ph.D. degree in control science and engineering.

His current research interests include real-time pricing, demand side response, and game theoretic approaches in electricity market.

Zheng-Yang Zeng received the B.Eng. degree from Tongji University, Shanghai, China, in 2009. He is presently pursuing the Ph.D. degree in control science and engineering.

His research interests include electric power network optimization and evolutionary computation.